JASETUI Vol. 1, No. 1 (2026): pp. (19–26)

Journal of Automotive Science and Engineering Technology
University of Ibadan, JASETUI

print-ISSN: 2587-**** https://journals.ui.edu.ng/index.php/JASETUI e-ISSN: 2587-****

Assessment of geospatial images fusion for enhanced pathloss prediction in mobile telecommunication systems

Ojo F. K[1,*], Jimoh A. A[1], Adeyemo Z. K[1],

[1] *Department of Electronic and Electrical Engineering, Faculty of Engineering and Technology, Ladoke Akintola University of Technology, Ogbomoso.*

ARTICLE INFO
Keywords:
Geospatial Images
Concatenate Input Features
Pathloss Prediction
Machine Learning Pathloss Model and Mobile Telecommunication Systems

ABSRACT

The development of accurate pathloss models is vital to the design of efficient telecommunication systems that ensure seamless and high-quality mobile signal coverage. Terrain characteristics significantly influence radio signal propagation, often causing distortions that affect signal quality. Therefore, incorporating these environmental features into pathloss prediction models is essential for realistic and reliable modeling. This study assessed a hybridized Convolutional Neural Network (CNN) model that concatenates the features of DenseNet121 and ResNet50 architectures to enhance learning capabilities. The model was trained using 3D geospatial terrain images fused with measured path loss values from various terrain types, including urban, suburban, and rural areas, across Ilorin, Kwara State, Nigeria. This fusion enables the model to capture both spatial and contextual terrain features that contribute to signal attenuation. The performance of the hybridised CNN-based pathloss model was compared with traditional empirical models and machine learning-based pathloss models, including Random Forest, XGBoost, and Transformer Vision. Results reveal that the hybridised CNN-based pathloss model delivers superior accuracy in predicting pathloss, achieving a Mean Square Error (MSE) of 7.35, a Root Mean Square Error (RMSE) of 8.295, and a coefficient of determination (R^2) of 0.80364. These metrics confirm the model's effectiveness and robustness in dynamic mobile environments, making it a reliable tool for modern telecommunication network planning and optimization.

1.0 Introduction

Reliable mobile signal reception is fundamentally dependent on the signal's ability to traverse and adapt to complex environmental landscapes that include both natural and man-made features [1]. Within the everyday environments of mobile users' homes, offices, schools, and public spaces, signal quality is significantly influenced by the distance from the nearest Base Transceiver Station (BTS) and the spatial distribution of surrounding terrain and structural features. These two primary factors, distance and environmental layout, are major contributors to signal degradation and increased pathloss. While deploying multiple BTSs has proven effective in mitigating the effects of long-distance signal transmission and in expanding coverage areas, terrain characteristics continue to present dominant challenges to signal propagation. Variations in terrain causes the signal to experience reflection, diffraction, and scattering, phenomena collectively referred to as multipath propagation [2].

These effects are highly dependent on the geographic and spatial arrangement of features in the signal's path. Urban environments, with their dense obstructions and vertical structures, differ significantly from suburban and rural areas in how they interact with mobile signals, leading to unique propagation challenges and limiting the generalisability of traditional pathloss models [3]. To capture the environmental influences on mobile signal behavior, researchers have long employed mathematical and statistical methods to create radio pathloss models that aim for higher precision [4].

Most of the widely used empirical, deterministic, and semi-empirical models incorporate terrain classifications and adjust predictions using terrain-specific correction factors. For instance, urban settings are typically modeled with assumptions about high population density, numerous high-rise structures, substantial signal diffraction, and scattering. In contrast, suburban areas are characterized by moderate building density and more open space, which results in different propagation behavior and necessitates adjusted correction factors. Rural environments, with their relatively flat, open landscapes and minimal obstructions, typically require the least signal correction. These models depend on correction factors derived through empirical field measurements, simulation data, or both. Such factors are crucial for refining pathloss predictions and enhancing their accuracy in practical network deployment scenarios. As the complexity of communication environments increases, so does the need for models that can dynamically adapt to real-world variations and better reflect the conditions that affect signal transmission [5].

The evolution of mobile telecommunications and the growing integration of Internet of Things (IoT) technologies have amplified the demand for more advanced, data-driven approaches to pathloss modeling. In response, this study explores the potential of leverag-

[0]*Corresponding author: David A. Fadare, da.fadare@ui.edu.ng
https://doi.org/**.****/jasetui.2026.0001
Received 20 January 2026; Received in revised form 22 April 2026; Accepted 5 May 2026
Available online 9 June 2026

ing geospatial imagery in the development of terrain-aware pathloss models, using a hybridized Convolutional Neural Network (CNN) framework. By combining DenseNet121 and ResNet50 CNN architectures, the study introduces a robust Machine Learning (ML) model capable of interpreting complex terrain patterns and predicting signal pathloss with greater accuracy. This hybridised CNN-based pathloss model is designed to learn from both structural terrain data and historical signal measurements, making it more adaptable to various propagation environments. Such an approach not only offers improved prediction capabilities over traditional models but also represents a significant advancement in the use of artificial intelligence for mobile network planning and optimization [6]. Ultimately, the study aims to contribute to the development of a more generalised, scalable, and precise pathloss prediction system, essential for meeting the increasing demand for reliable mobile communications networks in diverse and evolving environments. This article is organized as follows: the introduction provides the study's background, aim, and objectives.

The second section gives brief details of the evolution of hyperparameter's tuning in machine learning and convolutional neural network development. The methodology in section three details the hybridised model's development, data acquisition and processing, and the training and testing section of the hybridised CNN-based pathloss model. The results and discussions section presents the findings in evaluating and validating the model's predictability. Finally, the conclusions and recommendations for future work were presented.

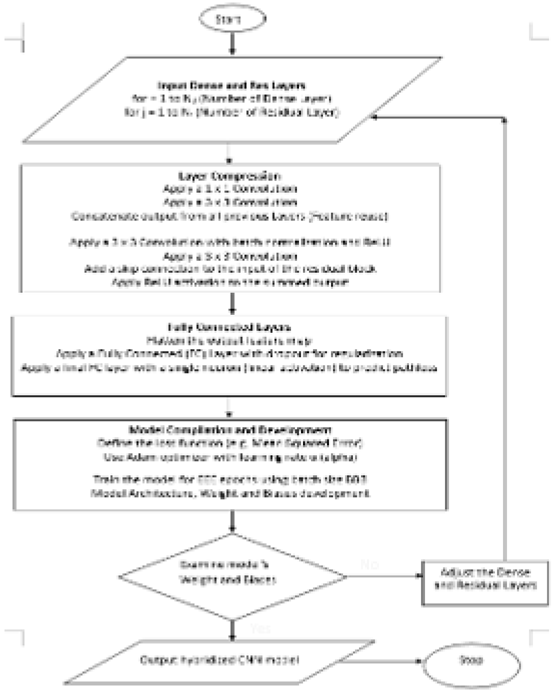

Figure 1: Flow Chat for the DenseNet and ResNet hybridization Process.

2.0 Evolution of Image Fusion in Pathloss Modelling

In the early stages of radio propagation research during the 1980s, pathloss modeling primarily relied on empirical models such as Okumura, Ericsson 999, and Hata, which were based on manually collected field measurements [7]. The 1990s marked a turning point with the introduction of high-resolution Digital Elevation Models (DEM) and Geographic Information Systems (GIS), which enabled more precise terrain and land cover data integration ([8], [9]). These innovations improved the prediction accuracy for urban, suburban, and rural environments by incorporating elevation and surface characteristics. However, these models remained constrained by static terrain inputs, limiting their responsiveness to real-time environmental variability [10]. The early 2000s introduced remote sensing and satellite imagery into the modeling process, enabling enhanced classification of land use and terrain features [11], [12]).

The emergence of Artificial Intelligence (AI) and multi-source data fusion technologies has ushered in a new era of pathloss modeling. Deep learning approaches, particularly Convolutional Neural Networks (CNNs) and Generative Adversarial Networks (GANs), now facilitate the automatic extraction of features from satellite and aerial imagery, integrating them with mobile network coverage data to significantly enhance prediction accuracy ([13], [6]). Fusion techniques that combine optical imagery, radar data, and LiDAR point clouds contribute to a more comprehensive representation of propagation environments [14].

Furthermore, real-time data sources such as Unmanned Aerial Vehicle (UAV)-based imagery, smart sensor networks, and crowd-sourced mobile signal strength data have enabled dynamic modeling systems that can adapt to rapidly changing environmental conditions [15]. These innovations mark a departure from traditional static models and allow for real-time responsiveness, increased granularity, and broader spatial coverage in signal prediction. The integration of AI with remote sensing technologies thus addresses many of the limitations previously encountered, supporting more reliable network planning and deployment in diverse environments.

Despite these advancements, recent machine learning-based pathloss studies still reveal notable limitations, particularly in the use of spatial data. Many recent efforts incorporate user terrain imagery in One-Dimensional (1D) or Two-Dimensional (2D) formats, utilizing features such as location, orientation, shape, and size of terrain objects for model training and testing. However, these approaches fall short of capturing the full geospatial complexity of the terrain, as they exclude Three-Dimensional (3D) representations that could more accurately reflect real-world topographical variations. In addition, most existing studies employ single CNN architectures, with limited exploration of hybridised models that could leverage the strengths of multiple CNN variants. This study addresses these gaps by:

(i) Developing a hybridised CNN-based architecture for improved pathloss modeling, combining DenseNet121 and ResNet50 architectures.

(ii) Implementing a 3D terrain geospatial image conversion framework to capture the full geospatial characteristics of the user environment's terrain features.

(iii) Evaluating the effectiveness of fused 3D geospatial imagery in enhancing prediction accuracy for mobile telecommunication systems.

Through the advancement of the modeling framework and the quality of terrain data used, this study contributes significantly to the evolution of pathloss modeling. It offers empirical insights into how 3D geospatial data fusion can revolutionize mobile signal prediction, thereby enabling more precise, adaptable, and intelligent mobile network planning in complex and dynamic propagation environments.

3.0 Materials and Methods

The methodology focuses on developing a hybridised CNN-based pathloss model architecture that combines DenseNet121 and ResNet50 variants to complement each other and enhance learning performance. The implementation leverages the efficiency of open-source tools available on Google Collaboratory, utilizing Python-based command scripts, as illustrated in the flowchart of Figure 1.

3.1 Field Measurement Work

Some selected mobile terrains routes were chatted across Ilorin, the Kwara State capital, and the routes span urban, suburban and rural areas of Ilorin Kwara State. Signal pathloss data were measured using RantCell professional and licensed application installed on Infinix Hot30 android mobile phone across all the mapped routes at an average speed of 40 km/hr during the field work, to mitigate against possible doppler frequency effect on the pathloss measured data [13]. The RantCell installed application's interface, and the traces of the mapped routes are as depicted in Figure 2.

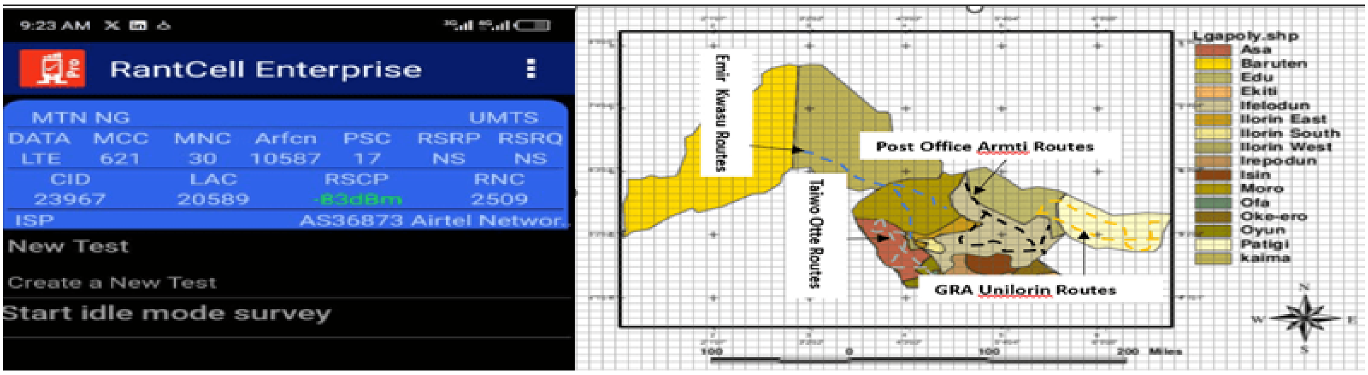

Figure 2: RantCell Mobile Signal Logger Interface and the traces of Measurement Routes Chatted during the Field Work Exercise.

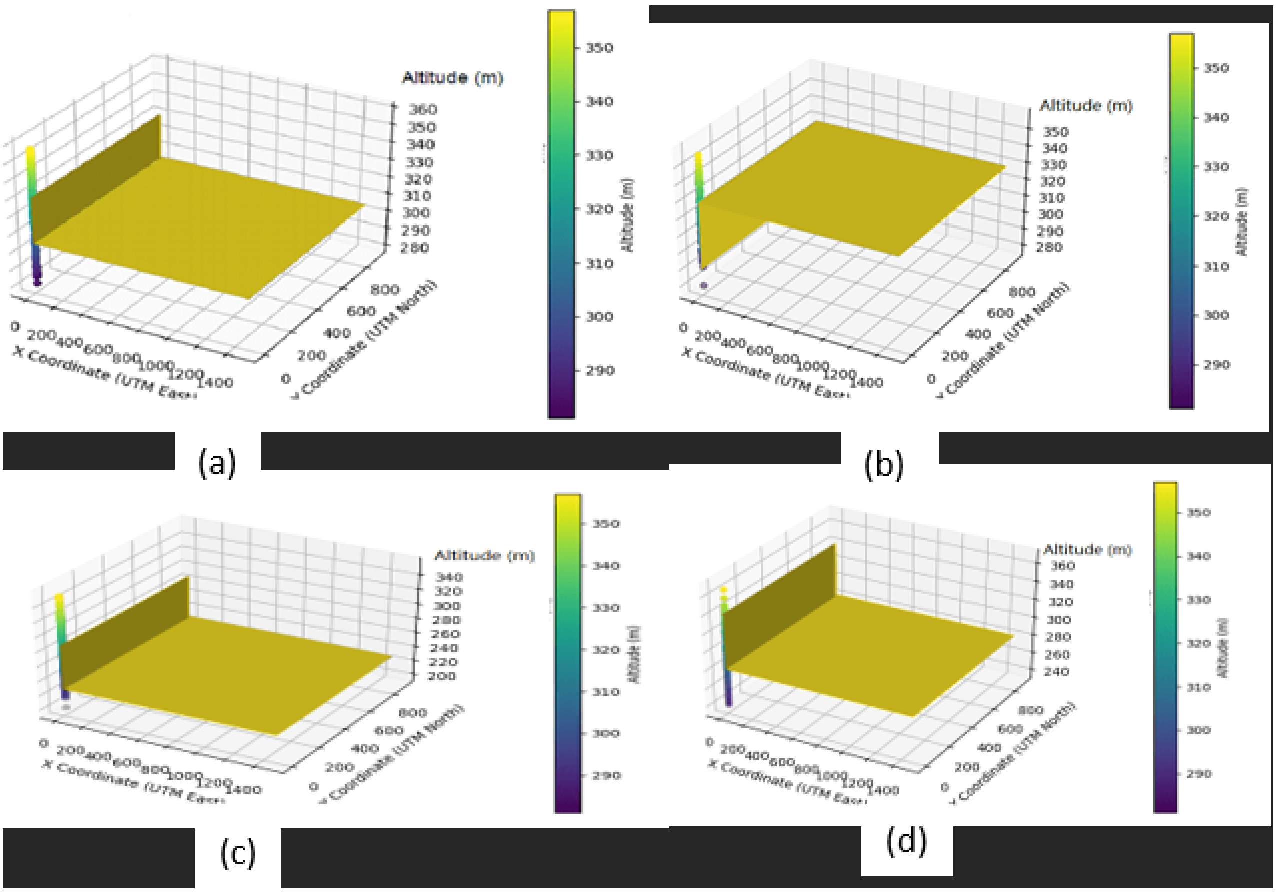

Figure 3: The overlaying process of the 2D Terrain Images with the UTM coordinates for (a) Emir Kwasu, (b) Taiwo Otte, (c) GRA Unilorin, (d) Post-Office Armti Measurement Routes.

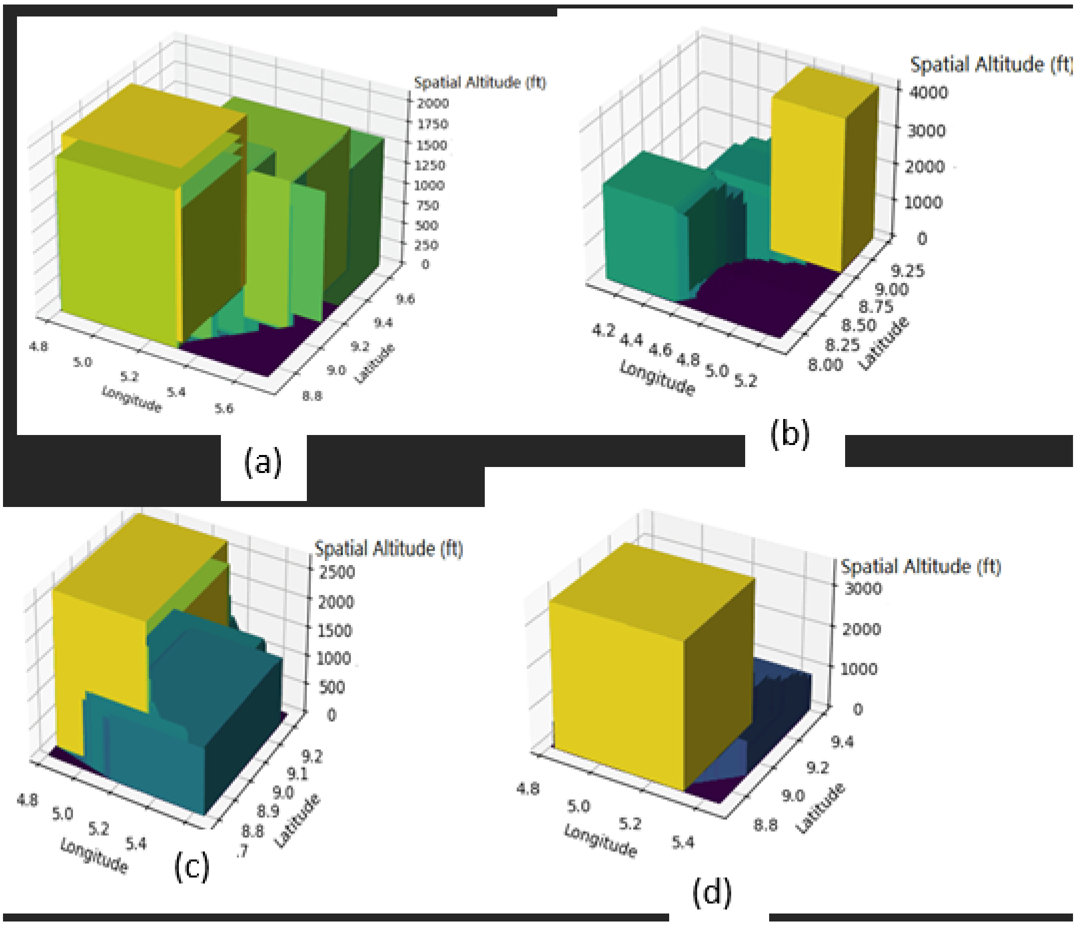

Figure 4: The Mean Geospatial 3D Histogram representation of the Terrain Images for (a) Emir Kwasu, (b) Taiwo Otte, (c) GRA Unilorin, (d) Post-Office Armti Measurement Routes.

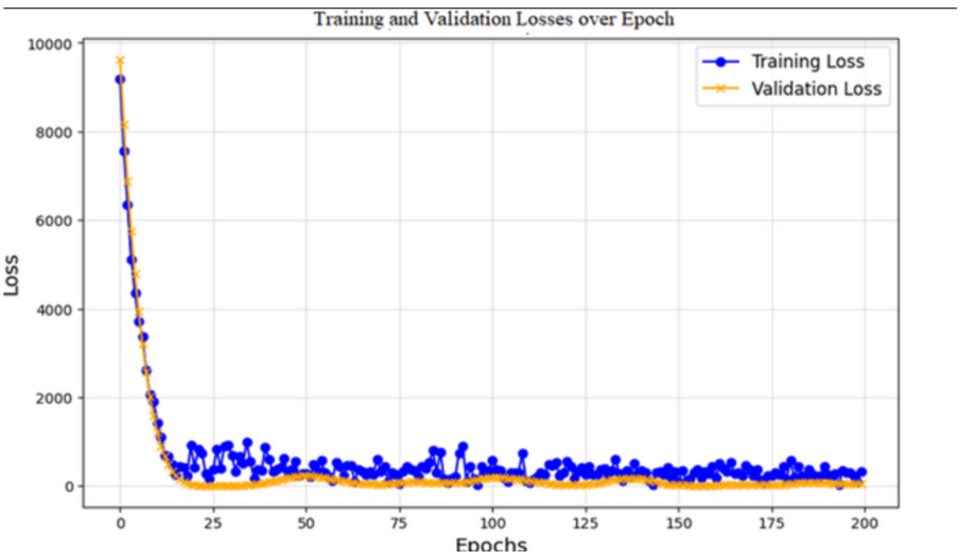

Figure 5: The hybridized CNN Improved Pathloss Model's Training Loss over Epochs

3.2 2D Images Conversion to 3D Geospatial Images

The terrain satellite images along the chatted field measurement routes were downloaded from Google Earth and overlayed with the Universal Transverse Mercator (UTM) cartesian coordinate [16] as inclination data. The overlaying processes are as depicted in 3, having the x-coordinates as (UTM East) and y-coordinates as (UTM North), and the altitude on the z-coordinates. These coordinates, respectively, give the east-west, north-south positions of the terrain features on the Earth's surface and their corresponding height above the datum (sea level).

Except for Fig. 3b, where the overlaying process started from a tall building, other routes have their overlaying process commencing from the lower floor. Furthermore, the significant output of this overlayed process is the generation of 3D histograms with geospatial dimensions as depicted in Fig. 4. The resulting 3D geospatial images classify and group terrain features with similar or approximate geospatial dimensions, presenting their mean representation in a concise 3D histogram format. This provides an aggregated view of terrain characteristics, making it easier for the hybridised CNN machine learning based architecture to capture and extract their influence on mobile signal propagation during training sessions.

3.3 Evaluation metrics

The hybridised CNN-based pathloss model was evaluated using the statistical and ML-based gauging metrics of mean error, Absolute mean error, Absolute error, Mean Squared Error and R-squared coefficient of determination.

(i) Mean error M_{error} It is the average of the errors spread between the measured pathloss values and the predicted path loss values. It helps quantify the average amount of errors in a set of predicted pathloss values [16] and it is as expressed in equation 1.

$$M_{\text{error}} = \frac{1}{n}\sum_{v=1}^{n}(M_v - P_v) \tag{1}$$

where, Mv and Pv are measured and predicted pathloss values, respectively.

(ii) Absolute mean error (Mean error *is the measure of the average magnitude of the errors between the predicted path loss values and the measured path loss values. It is similar to the mean error, but it takes the absolute value of the differences, making it always positive [17]. The mathematical expression is as expressed in equation 2*

$$A_{m\text{-}error} = \frac{1}{n}\left|\sum_{v=1}^{n}(M_v - P_v)\right| \tag{2}$$

where n is the number of occurrences, Mv and Pv are as defined in equation 1.

(iii) Mean Absolute Error (MAE) It measures the average magnitude of errors in path loss predictions, without considering their direction. It gives an overview of how much the predicted path loss values deviate from the actual measured path loss values [18].

$$MAE = \frac{1}{n}\sum_{i=1}^{n}|y_i - \hat{y}_i| \tag{3}$$

where:

- *n is the number of data points,*
- *y_i is the actual measured path loss value,*
- *$\hat{y}_i$ is the predicted path loss value, and*
- *$|y_i - \hat{y}_i|$ represents the absolute error for each path loss prediction.*

Lower MAE values indicate better model performance. The MAE is easy to interpret because it represents the average prediction error in the same units as the output variable.

(iv) Mean Squared Error (MSE) it computes the average squared difference between predicted and actual values. It penalizes larger errors more heavily than MAE due to squaring [19].

$$MSE = \frac{1}{n}\sum_{i=1}^{n}(y_i - \hat{y}_i)^2 \tag{4}$$

where n, y_i, and $\hat{y}_i$ are as defined in Equation 3. The term $(y_i - \hat{y}_i)^2$ represents the squared error for each predicted path loss value. Lower MSE values indicate better prediction accuracy. However, because the errors are squared, the MSE metric amplifies the impact of outliers because errors are squared.

(v) R-squared – coefficient of determination $(R^2) measureshowwellthemodele$ value ranges from 0 to 1, where a value of 1 indicates a perfect fit, while a value of 0 indicates a poor fit [20].

$$R^2 = 1 - \frac{\sum_{i=1}^{n}(y_i - \hat{y}_i)^2}{\sum_{i=1}^{n}(y_i - \bar{y})^2} \tag{5}$$

where n, y_i, and $\hat{y}_i$ are as defined in Equation (3.6), $\bar{y}$ is the mean of the actual measured path loss values, $\sum_{i=1}^{n}(y_i - \hat{y}_i)^2$ is the residual sum of squares, and $\sum_{i=1}^{n}(y_i - \bar{y})^2$ is the total sum of squares. The values of R^2 range between 0 and 1, where 1 indicates a perfect fit and 0 indicates a poor fit.

4.0 Results and Discussions

The concatenated input parameters totaling 32,988,357 were used to train the hybridised CNN-based pathloss model, occupying approximately 125.84 MB of memory; of these input parameters, 30,625,216 (116.83 MB) are trainable, indicating the model's capacity for learning complex patterns during retraining. The 787,713 non-trainable parameters (3.00 MB) suggest partial fine-tuning with some pre-trained layers frozen. The training summaries are as presented in Table 1.

Additionally, the model includes 1,575,428 optimizer parameters (6.01 MB) that support efficient weight updates during training. This parameter breakdown reflects the model's computational demands and optimization strategy for effective signal pathloss prediction. Early training stages showed a sharp decline in both training and validation losses as depicted in Fig. 5, indicating rapid learning, with losses stabilizing around epoch 25. Some oscillations in the training loss suggested minor instability, potentially due to high learning rates and insufficient regularization, although overfitting remained minimal. Performance metrics, including Mean Absolute Error (MAE), Mean Squared Error (MSE), and R-squared (R^2), were tracked over 200 epochs. Initially, the model exhibited poor performance (e.g., MAE of 29.18 and negative R^2 at epoch 25), but these metrics improved steadily as epoch increases.

In Table 2, at epoch 150, the model achieved an MAE of 9.01, MSE of 18.54, and an R^2 nearing zero (–0.1), indicating improved prediction capability and convergence. At epoch 200, optimal performance was reached with MAE reduced to 2.08, MSE to 7.35, and R^2 rising to 0.8, reflecting strong generalisation to unseen data. Although training time per step increases progressively from 541 ms at epoch 25 to 593 ms at epoch 200, this was attributed to increasing model complexity and was considered a reasonable trade-off for the improved accuracy. Overall, the model demonstrated robust learning behaviour, low prediction error, and strong generalisation ability, validating its effectiveness for signal pathloss prediction in dynamic telecommunications environments.

In Table **??**(a), **??**(b), and 3(c) depicts the comparison of the hybridised CNN-based pathloss model against three traditional pathloss models of; Davidson, COST231-Hata, and IEEE at 900 MHz, 1800 MHz and 2100 MHz to assess the generalisation of the predictability of the hybridised CNN-based pathloss model across the prominent three frequencies of mobile communication. The hybridized CNN model achieved the best results across all metrics, with a consistently low error margin. Its SE was recorded at 153, significantly outperforming the Davidson model, which had large negative SE values ranging from -4357 to -5565.

Table 1: Presents the Summary of Training of the hybridized CNN-based Model's Architecture

S/N	Layer (Type)	Output Shape	Parameters
1	Input Layer	(None, 224, 224, 3)	0
2	DenseNet121 (Functional)	(None, 7, 7, 1024)	7,037,504
3	ResNet50 (Functional)	(None, 7, 7, 2048)	23,587,712
4	GlobalAveragePooling2D	(None, 1024)	0
5	GlobalAveragePooling2D	(None, 2048)	0
6	Concatenate	(None, 3072)	0
7	Input Layer (Numerical Features)	(None, 3)	0
8	Concatenate	(None, 3075)	0
9	Dense (256 neurons)	(None, 256)	787,456
10	Dropout	(None, 256)	0
11	Dense (Output Layer)	(None, 1)	257
Total Parameters			32,988,357
Trainable Parameters			30,625,216
Non-trainable Parameters			787,713
Optimizer Parameters			1,575,428

Table 2: The Metrics' Progression for the hybridized CNN-based Pathloss Model during Training

S/N	Epochs	MAE	MSE	R^2	millisec/step
1	25	29.18	50.28	-6.64	541
2	50	25.15	34.43	-6.01	549
3	75	26.45	30.14	-5.30	543
4	100	20.27	26.76	-5.10	553
5	125	15.01	20.14	-1.60	535
6	150	9.01	18.54	-0.10	546
7	175	4.07	11.11	0.50	537
8	200	2.08	7.35	0.80	593

Note: Epoch represents the number of times the CNN-based pathloss model architecture processes the entire training dataset during training.

Table 3: (a) Comparison of Predicted Pathloss Metrics across Models at 900 MHz

S/N	Gauging Metrics	Davidson	IEEE	COST231-Hata	Hybridised CNN
1	Sum of Errors (SE)	-4357	-2480	-3971	153
2	Mean Error (ME)	-57	-33	-52	2
3	Absolute Mean Error (AME)	73	44	65	2

IEEE – Institute of Electrical and Electronics Engineers; COST231 – European Cooperation in Science and Technology (COST) Action 231.

Table 3: (b) Comparison of Predicted Pathloss Metrics across Models at 1800 MHz

S/N	Gauging Metrics	Davidson	IEEE	COST231-Hata	Hybridised CNN
1	Sum of Errors (SE)	-5346	-3167	-4746	153
2	Mean Error (ME)	-70	-42	-62	2
3	Absolute Mean Error (AME)	73	44	65	2

Note: IEEE = Institute of Electrical and Electronics Engineers; COST231 = European Cooperation in Science and Technology (COST) Action 231.

Table 3: (c) Comparison of Predicted Pathloss Metrics across Models at 2100 MHz

S/N	Gauging Metrics	Davidson	IEEE	COST231-Hata	Hybridised CNN
1	Sum of Errors (SE)	-5565	-3319	-4919	153
2	Mean Error (ME)	-73	-44	-65	2
3	Absolute Mean Error (AME)	73	44	65	2

Note: IEEE = Institute of Electrical and Electronics Engineers; COST231 = European Cooperation in Science and Technology (COST) Action 231.

Similarly, the hybridised CNN-based pathloss model maintained a minimal ME of 2 at all frequencies, while the traditional models, particularly Davidson, recorded much larger negative values, indicating persistent underprediction. These findings highlight that the hybridized CNN model is significantly more robust and adaptable across different frequency bands. Unlike traditional models, it effectively handles variations in propagation environments, maintaining prediction accuracy even as the frequency increases. Therefore, the study went further to assess the hybridised CNN-based pathloss model against other widely used ML-based pathloss models.

The training session of the hybridised CNN-based pathloss model with other ML-based pathloss models of (Random Forest, XGBoost and Transformer) were conducted on Google Collaboratory. The training results of Table 4, of ME, MSE, RMSE and R^2 were used to assess the models.

The results in Table 4, indicate the hybridised CNN-based pathloss model delivers the best performance amongst the three ML-based pathloss models, achieving the best fit values of (MSE: 2.82 RMSE 8.29) and highest coefficient of determination (R^2: 0.80), confirming its superior accuracy [19]. The RF model follow with moderate performance with an RMSE of 8.19 and R^2 of 0.45. XGBoost performs slightly below RF with an RMSE value of 8.72 and R^2 of 0.37. The Transformer model shows the weakest performance with the least gauging metrics of MSE: 96.05, RMSE: 9.80 and R^2 of 0.16, reflecting limited predictive capability.

5. Conclusions and Future Work

In conclusion, this study highlights the effectiveness of combining advanced neural network architectures with fused 3D geospatial image data to enhance the predictive accuracy of the hybridised CNN-based pathloss model. The hybridised CNN-based pathloss model's performance validated the integration of geospatial image fusion in developing a predictive pathloss model using a hybridized Convolutional Neural Network (CNN) architecture combining DenseNet121 and ResNet50 variants. The findings demonstrate that image-based pathloss modelling provides a more robust and accurate prediction framework compared to conventional methods. Specifically, the hybridized CNN-based pathloss model significantly outperforms three widely referenced empirical pathloss models—Davidson, COST231-Hata, and IEEE across three operating frequencies of 900 MHz, 1800 MHz, and 2100 MHz. These results validate the model's ability to adapt to frequency-dependent variations and complex propagation environments.

Furthermore, the architectural depth and connectivity of the DenseNet121 and ResNet50 combination provided a rich and efficient learning structure, contributing to the model's superior performance. This was further evident when the hybridized CNN model was compared against three prominent ML-based models: Random Forest, XGBoost, and Transformer Vision. Amongst all, the hybridized CNN-based pathloss model consistently achieved the lowest prediction errors and the highest R^2 values, underscoring its superior generalisation capability and accuracy.

The success of the hybridization approach demonstrates its potential as a valuable tool for future telecommunication planning, especially in diverse and dynamic radio propagation environments. This study not only reinforces the importance of data fusion and deep learning in signal modelling but also provides a strong foundation for further development in intelligent wireless network design.

Table 4: Comparison of Predicted Pathloss Metrics across Models at 2100 MHz

S/N	Metric	XGBoost	RF	Transf.	CNN
1	ME	-0.2276	-0.0694	-0.0587	-0.0125
2	MSE	76.1131	67.2043	96.0593	2.8252
3	RMSE	8.7243	8.1978	9.8010	8.2958
4	R^2	0.3782	0.4510	0.1683	0.8036

Note: XGBoost = Extreme Gradient Boosting; RF = Random Forest; CNN = Convolutional Neural Network; Transf. = Transformer.

References

[1] R. N. Clarke, "Expanding mobile wireless capacity: The challenges presented by technology and economics," *Telecommunications Policy*, vol. 38, no. 8–9, pp. 693–708, 2014.

[2] A. A. Jimoh, N. T. Surajudeen-Bakinde, N. Faruk, and O. W. Bello, "Assessment of multipath and shadowing effects on uhf band in built-up environments," *Abubakar Tafawa Balewa University Journal of Environment Technology*, vol. 10, no. 1, pp. 1–11, 2017.

[3] A. A. Jimoh, O. A. Lawal, Z. A. Abdulkadir, and K. Lateef, "A priori study of multi dwelling unit effect on 4g mobile network in ilorin metropolis," *International Journal of Innovative Research and Advanced Studies*, vol. 9, no. 8, pp. 1–6, 2022.

[4] P. E. Afolabi, S. O. Ikubanni, B. O. Adebesin, S. J. Adebiyi, and E. F. Adeleke, "Effects of weather parameters on signal attenuation: A brief review," in *2024 International Conference on Science, Engineering and Business for Driving Sustainable Development Goals (SEB4SDG)*, 2024, pp. 1–5.

[5] H. Qi, Y. Wang, and X. Liu, "3d regnet: Deep learning model for covid-19 diagnosis on chest ct image," 2021.

[6] M. F. Al Hakim and B. Prasetiyo, "Cnn-ml stacking for better classification of rice leaf diseases," in *2024 IEEE International Conference on Artificial Intelligence and Mechatronics Systems (AIMS)*, 2024, pp. 1–5.

[7] A. A. Jimoh, N. T. Surajudeen-Bakinde, N. Faruk, A. A. Ayeni, O. O. Obiyemi, and O. W. Bello, "Performance analysis of empirical path loss models in vhf and uhf bands," in *6th International Conference on Information and Communication Systems*, 2015, pp. 194–199.

[8] N. Baccour, D. Puccinelli, T. Voigt, A. Koubaa, C. Noda, H. Fotouhi, M. Alves, H. Youssef, M. A. Zuniga, C. A. Boano, and K. Römer, "External radio interference," in *Radio Link Quality Estimation in Low-Power Wireless Networks*. Springer International Publishing, 2013, pp. 21–63.

[9] M. Cheffena and M. Mohamed, "Empirical path loss models for wireless sensor network deployment in snowy environments," *IEEE Antennas and Wireless Propagation Letters*, pp. 1–1, 2017.

[10] D. Fazilova, "Uzbekistan's coordinate system transformation from cs42 to wgs84 using distortion grid model," *Geodesy and Geodynamics*, vol. 13, no. 1, pp. 24–30, 2022.

[11] M. K. Elmezughi, T. J. Afullo, and N. O. Oyie, "Performance study of path loss models at 14, 18, and 22 ghz in an indoor corridor environment for wireless communications," *SAIEE Africa Research Journal*, vol. 112, no. 1, pp. 32–45, 2021.

[12] M. Sousa, P. Vieira, M. P. Queluz, and A. Rodrigues, "An ubiquitous 2.6 ghz radio propagation model for wireless networks using self-supervised learning from satellite images," *IEEE Access*, vol. 10, pp. 78 597–78 615, 2022.

[13] A. Abdulkarim, N. Faruk, E. Alozie, O. A. Sowande, I.-F. Y. Olayinka, A. D. Usman, K. S. Adewole, A. A. Oloyede, H. Chiroma, S. Garba, A. L. Imoize, A. Musa, and L. S. Taura, "Application of machine learning algorithms to path loss modeling: A review," in *2022 5th Information Technology for Education and Development (ITED)*, 2022, pp. 1–6.

[14] I. Yazici, E. Özkan, and E. Gures, "Enhancing path loss prediction through explainable machine learning approach," in *2024 11th International Conference on Wireless Networks and Mobile Communications (WINCOM)*, 2024, pp. 1–5.

[15] Institute of Electrical and Electronics Engineers and IEEE Communications Society, Eds., *2014 Eleventh Annual IEEE International Conference on Sensing, Communication, and Networking Workshops (SECON Workshops 2014)*. Singapore: IEEE, 2014.

[16] S. McGrath, X. Zhao, R. Steele, B. D. Thombs, A. Benedetti, Y. Zhang *et al.*, "Estimating the sample mean and standard deviation from commonly reported quantiles in meta-analysis," *Statistical Methods in Medical Research*, vol. 29, no. 9, pp. 2520–2537, 2020.

[17] Z. Fabián, "Mean, mode or median? the score mean," *Communications in Statistics - Theory and Methods*, vol. 50, no. 10, pp. 2360–2370, 2021.

[18] V. M. Patro and P. M. Ranjan, "Augmenting weighted average with confusion matrix to enhance classification accuracy," *Transactions on Machine Learning and Artificial Intelligence*, vol. 2, no. 4, pp. 34–38, 2014.

[19] M. Heydarian, T. E. Doyle, and R. Samavi, "Mlcm: Multi-label confusion matrix," *IEEE Access*, vol. 10, pp. 19 083–19 095, 2022.

[20] X. Deng, Q. Liu, Y. Deng, and S. Mahadevan, "An improved method to construct basic probability assignment based on the confusion matrix for classification problem," *Information Sciences*, vol. 340–341, pp. 250–261, 2016.